

# A Passivity Control Strategy for VSC-HVDC Connected Large Scale Wind Power

Xinming Fan, Lin Guan, Chengjun Xia, Jianming He

**Abstract**--For wind farm connection VSC-HVDC transmission has obvious technical and economic advantages, but concentrated integration of large scale wind power requires stronger robustness. Based on the mathematical model of VSC-HVDC in abc frame, the Euler-Lagrange mathematical model of voltage-source-converter(VSC) in d-q rotating frame is built and the strict passivity of VSC is proved. Based on the energy dissipativity of VSC, energy storage function is established by using state error and it is used as Lyapunov function, VSC-HVDC is astringed to expected stable equilibrium point rapidly by damping addition. The passivity controller is designed according to expected equilibrium point, state variable and state error, and decoupling control for various variable is achieved. With different operation conditions, VSC-HVDC and its control system are simulated by software PSCAD/EMTDC, the results show that the proposed control strategy has good performance and strong robustness either in dynamic state or steady state.

**Index Terms**--large scale wind power, VSC-HVDC, passivity, EL mathematical model, error storage function, decoupling control.

## I. INTRODUCTION

Wind power is the main alternative energy when every country fulfils its renewable energy development goals. By the end of 2010, 196630MW wind power has been installed all over the world[1]. Meanwhile large scale wind farms of hundreds of MWs of power are developed in many countries around the world. With the development of wind turbine and power electronics technologies, wind farms are being changed from small-sized, distributed and locally-connected to large-scale, highly concentrated and remote high voltage transmission[2][3]. HVDC with voltage source converter (VSC-HVDC) has fine dynamic characteristic and transmission flexibility, furthermore, it improves the stability of power system [4]-[7]. In addition, in comparison with other solutions VSC-HVDC is more economical for hundred megawatts wind farm[8][9]. Therefore, VSC-HVDC has obvious technical and economic advantages for the connection

of large scale wind farm.

The VSC-HVDC system can be operated in three modes: 1) constant DC voltage control mode; 2) constant active and reactive power control mode; and 3) constant AC voltage control mode[10]. Therefore the control of DC/AC voltage and power is very important, especially at least one of the converter stations has to control the DC voltage to make the active power balanced and the DC voltage stable[11][12]. However four control inputs of the VSC-HVDC transmission link and their interaction makes the system a truly nonlinear multiple-input multiple-output control system. Voltage vector oriented double closed-loop PID control based on synchronous rotating reference frame is the most common method to solve the nonlinear problem[13][14]. Moreover, some advanced control strategies are applied to VSC-HVDC transmission link that include feedback linearization and sliding mode control to achieve decoupled control of multiple-input multiple-output variable[10], adaptive control based on backstepping method to improve the dynamic characteristic of VSC-HVDC[15], fuzzy-PI inner loop control applied to voltage source converter[16], and PID neural network sliding mode controller for voltage source converter[17]. But it is difficult to achieve ideal effects because of the multivariable structure and highly coupled nonlinearity of the VSC-HVDC system.

Passivity control is an emerging nonlinear control theory based on the energy dissipation of system[18][19], and was applied to many areas successfully [20][21]. In this paper the passivity controller of VSC is deisigned based on Euler-lagrange(EL) mathematical mode of VSC-HVDC. The control strategy makes the VSC-HVDC transmission linked large scale wind farm has better static and dynamic performance and stronger robustness. The simulation results under different operation conditions show its superiority.

## II. TOPOLOGY AND MATHEMATICAL MODEL OF THE VSC-HVDC TRANSMISSION SYSTEM

The single line diagram of the VSC-HVDC transmission connected a wind farm is shown in Fig.1. Wind farm is connected to the sending end VSC by a transformer, the receiving end VSC is linked to the main network, and both VSC connected to each other by long distance DC transmission line. The detailed structure of VSC is shown in Fig.2, the transformer reactance and power loss are equivalent to L and R, and the parameters of the three phase circuits are assumed to be identical.  $U_{sa}$ ,  $U_{sb}$  and  $U_{sc}$  are phase voltage at

---

This work was supported by the national high technology research and development program of China (863 Program) (No. 2011AA05A102).

Xinming Fan is with School of Electric Power, South China University of Technology, Guangzhou 510641, China (e-mail:fanxinming1230@126.com).

Lin Guan is with School of Electric Power, South China University of Technology, Guangzhou 510641, China (e-mail: lguan@scut.edu.cn).

Chengjun Xia is with School of Electric Power, South China University of Technology, Guangzhou 510641, China (e-mail: cjxia@scut.edu.cn).

Jianming He is with School of Electric Power, South China University of Technology, Guangzhou 510641, China.

the point of common coupling (PCC),  $i_a$ ,  $i_b$  and  $i_c$  are line current at PCC.  $u_a$ ,  $u_b$  and  $u_c$  are phase voltage at the AC side of the converter,  $u_{dc}$  is the dc voltage,  $i_{dc}$  is DC current in the DC transmission line.

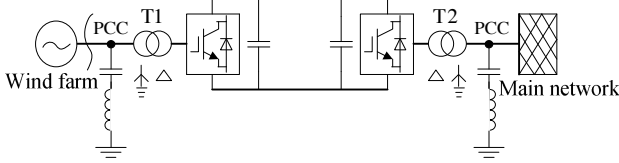


Fig.1 Wind farm VSC-HVDC connection topology

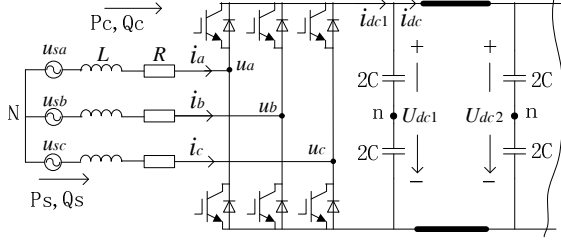


Fig.2 VSC-HVDC circuit topology

The mathematical model of the VSC-HVDC VSC in the three phase static frame is

$$\begin{cases} L \frac{di_a}{dt} = u_{sa} - u_a - Ri_a = u_{sa} - u_{dc}(s_a - \frac{1}{3} \sum_{j=a,b,c} s_j) - Ri_a \\ L \frac{di_b}{dt} = u_{sb} - u_b - Ri_b = u_{sb} - u_{dc}(s_b - \frac{1}{3} \sum_{j=a,b,c} s_j) - Ri_b \\ L \frac{di_c}{dt} = u_{sc} - u_c - Ri_c = u_{sc} - u_{dc}(s_c - \frac{1}{3} \sum_{j=a,b,c} s_j) - Ri_c \\ c \frac{du_{dc}}{dt} = s_a i_a + s_b i_b + s_c i_c - i_{dc} \end{cases} \quad (1)$$

Where  $s_j$  ( $j=a,b,c$ ) is the logic switch function, when  $s_j = 1$  the upper bridge arm is conductive and lower bridge arm is turn-off, when  $s_j = 0$  the contrary is the case. By Park transformation matrix and its inverse matrix, equation (1) can be transformed to mathematical model in d-q synchronous rotating frame as equation (2)

$$\begin{cases} L \frac{di_d}{dt} = u_{sd} - u_d - Ri_d - \omega Li_q = u_{sd} - s_d u_{dc} - Ri_d - \omega Li_q \\ L \frac{di_q}{dt} = u_{sq} - u_q - Ri_q + \omega Li_d = u_{sq} - s_q u_{dc} - Ri_q + \omega Li_d \\ \frac{2}{3} c \frac{du_{dc}}{dt} = s_d i_d + s_q i_q - \frac{2}{3} i_{dc} \end{cases} \quad (2)$$

Where  $s_d$  and  $s_q$  represent the d and q components of the switch function,  $u_{sd}$  and  $u_{sq}$  are the d and q components of the voltage at PCC,  $u_d$  and  $u_q$  are the d and q components of the voltage at AC side of the converter. The active power  $p_s$  and reactive power  $q_s$  in the d-q synchronous rotating coordinates are

$$\begin{cases} p_s = \frac{3}{2} (u_{sd} i_d + u_{sq} i_q) \\ q_s = \frac{3}{2} (u_{sd} i_q - u_{sq} i_d) \end{cases} \quad (3)$$

When d axis is oriented at the vector of the voltage at PCC, then  $u_{sq} = 0$ , and  $p_s = \frac{3}{2} u_{sd} i_d$ ,  $q_s = \frac{3}{2} u_{sd} i_q$ , so controlling the  $i_d$  and  $i_q$  respectively can realize the decoupled control of  $p_s$  and  $q_s$ .

### III. EL MODEL OF VSC-HVDC CONVERTER

Transform the equation (2) to the form of (4)

$$\begin{bmatrix} L & 0 & 0 \\ 0 & L & 0 \\ 0 & 0 & \frac{2}{3} C \end{bmatrix} \begin{bmatrix} \frac{di_d}{dt} \\ \frac{di_q}{dt} \\ \frac{du_{dc}}{dt} \end{bmatrix} + \begin{bmatrix} R & 0 & 0 \\ 0 & R & 0 \\ 0 & 0 & 2/3R_{dc} \end{bmatrix} \begin{bmatrix} i_d \\ i_q \\ u_{dc} \end{bmatrix} + \begin{bmatrix} 0 & \omega L & s_d \\ -\omega L & 0 & s_q \\ -s_d & -s_q & 0 \end{bmatrix} \begin{bmatrix} i_d \\ i_q \\ u_{dc} \end{bmatrix} = \begin{bmatrix} u_{sd} \\ u_{sq} \\ 0 \end{bmatrix} \quad (4)$$

Where  $R_{dc} = u_{dc} / i_{dc}$  is the equivalent resistance at the DC side of the converter. According to the Euler-lagrange Equation[22][20], Equation (4) has the form

$$M\dot{x} + \mathfrak{R}x + Jx = u \quad (5)$$

Where  $M$  is the positive definite diagonal matrix;  $\mathfrak{R}$  is the positive definite matrix and characterizes the passivity;  $J$  is antisymmetric matrix,  $J = -J^T$ , and reflects the interconnection character of state variable;  $u$  is the control inputs. According to equation (4), the detailed expressions of above matrixes are

$$M = \begin{bmatrix} L & 0 & 0 \\ 0 & L & 0 \\ 0 & 0 & \frac{2}{3} C \end{bmatrix}, \quad \mathfrak{R} = \begin{bmatrix} R & 0 & 0 \\ 0 & R & 0 \\ 0 & 0 & 2/(3R_{dc}) \end{bmatrix},$$

$$J = \begin{bmatrix} 0 & \omega L & s_d \\ -\omega L & 0 & s_q \\ -s_d & -s_q & 0 \end{bmatrix}, \quad x = \begin{bmatrix} x_1 \\ x_2 \\ x_3 \end{bmatrix} = \begin{bmatrix} i_d \\ i_q \\ u_{dc} \end{bmatrix}, \quad u = \begin{bmatrix} u_{sd} \\ u_{sq} \\ 0 \end{bmatrix}.$$

Assuming that the energy storage function of voltage source converter is  $H = \frac{1}{2} x^T M x$ , then deducing by equation (5) may get

$$\dot{H} = x^T M \dot{x} = x^T (u - Jx - \mathfrak{R}x) = x^T u - x^T \mathfrak{R}x \quad (6)$$

Now makes the output  $y = x$ , the energy supply rate  $s(u, y) = u^T y$ , positive definite function is  $Q(x) = x^T \mathfrak{R}x$ , then the energy storage of the system is

$$H[x(t)] - H[x(0)] \leq \int_0^t u^T y d\tau - \int_0^t x^T \mathfrak{R}x d\tau \quad (7)$$

or

$$\dot{H} \leq u^T y - Q(x) \quad (8)$$

Consequently, the VSC is strictly passive. The attenuation characteristics of energy function just reflects stability of Lyapunov and energy function is exactly used as Lyapunov function.

### IV. PASSIVITY CONTROLLER DESIGNED FOR CONVERTER

When VSC-HVDC converter is at steady state, the variables of expected stable equilibrium points  $x_1^* = i_d^*$ ,  $x_2^* = i_q^*$ ,  $x_3^* = u_{dc}^*$ . The error storage function is chosen as  $H_e = \frac{1}{2} x_e^T M x_e$ , and  $x_e = x - x^*$ , from equation (5) we obtain

$$M\dot{x}_e + \mathfrak{R}x_e + Jx_e = u - (M\dot{x}^* + \mathfrak{R}x^* + Jx^*) \quad (9)$$

To make the error storage function equal to zero and the system astringe to expected equilibrium point quickly, the energy dissipation should be accelerated and damping is added. The damping is

$$\mathfrak{R}_d = (\mathfrak{R} + \mathfrak{R}_a) \quad (10)$$

Where  $\mathfrak{R}_a$  is positive definite matrix, then equation (9) is transformed to

$$\begin{aligned} M\dot{x}_e + \mathfrak{R}_d x_e + Jx_e \\ = u - (M\dot{x}^* + \mathfrak{R}x^* + Jx^*) + \mathfrak{R}_a x_e \end{aligned} \quad (11)$$

Make the equation

$$u - (M\dot{x}^* + \mathfrak{R}x^* + Jx_e + Jx^*) + \mathfrak{R}_a x_e = 0 \quad (12)$$

And  $M\dot{x}_e + \mathfrak{R}_d x_e = 0$ , then

$$\dot{H}_e = x_e^T M\dot{x}_e = -x_e^T \mathfrak{R}_d x_e < 0 \quad (13)$$

Equation (13) shows the error storage function can astringe quickly and its convergence rate is influenced by  $\mathfrak{R}_a$ . According to equation (12), gets the passivity control law and it is

$$\begin{cases} S_d u_{dc} = u_{sd} + R_a i_d - (R + R_a) i_d^* - \omega L i_q \\ S_q u_{dc} = u_{sq} + R_a i_q - (R + R_a) i_q^* + \omega L i_d \end{cases} \quad (14)$$

Equation (14) could be written in

$$\begin{cases} u_d = u_{sd} + R_a i_d - (R + R_a) i_d^* - \omega L i_q \\ u_q = u_{sq} + R_a i_q - (R + R_a) i_q^* + \omega L i_d \end{cases} \quad (15)$$

Therefore the voltage at the AC side of converter can be get from equation (15). Substituting equation (14) in equation (2) gets

$$\begin{cases} L \frac{di_d}{dt} = (R + R_a)(i_d^* - i_d) \\ L \frac{di_q}{dt} = (R + R_a)(i_q^* - i_q) \\ c \frac{du_{dc}}{dt} = (u_{dc}^* - u_{dc}) / R_{dc} + 3R_a(u_{dc}^* - u_{dc}) / 2 \end{cases} \quad (16)$$

Equation (16) shows  $i_d$ ,  $i_q$  and  $u_{dc}$  can be stable at expected equilibrium points when  $\mathfrak{R}_a$  is big enough. In addition, it shows the control law can achieve decoupled control for  $i_d$ ,  $i_q$  and  $u_{dc}$ .  $i_d^*$  and  $i_q^*$  can be got from the outer control loop. In order to facilitate active power setting and voltage control for wind farm, active power and constant voltage control are used at the sending end, Fig.3 shows the control diagram.

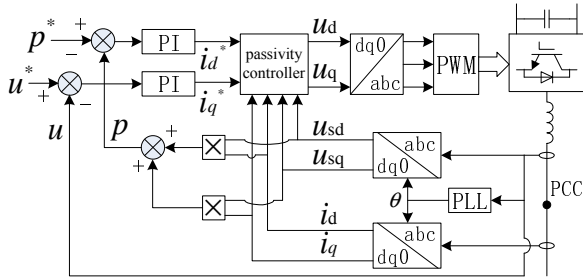


Fig.3 Passivity decoupled control strategy for sending-end VSC

To meet active power balance and DC voltage stability, constant DC voltage and constant AC voltage controls are used at receiving end, Fig.4 shows the control diagram.

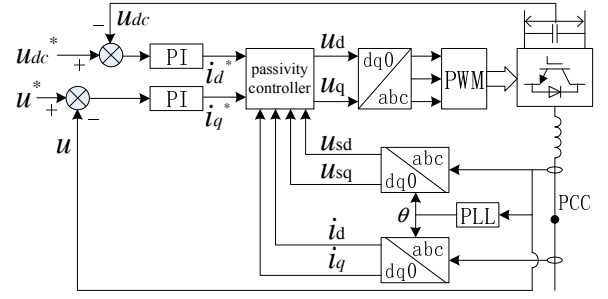
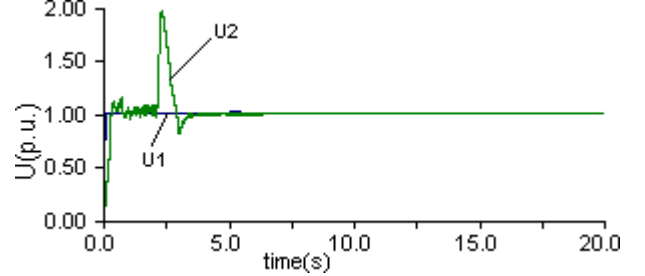


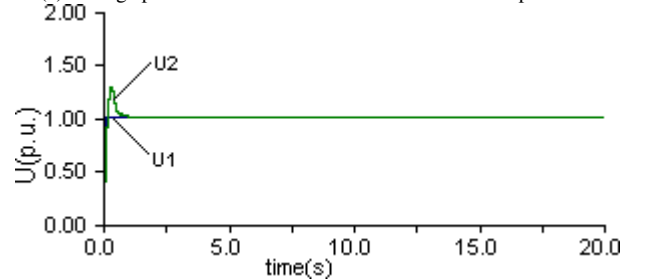
Fig.4 Passivity decoupled control strategy for receiving-end VSC

## V. SIMULATION AND ANALYSIS

In order to verify the validity and superiority of the proposed control strategy, the VSC-HVDC transmission linked wind farm and its control strategy are modeled and simulated by software PSCAD/EMTDC. The rated DC voltage of the VSC-HVDC link is  $\pm 160$  kV, the converter capacity is 200 MVA and the base capacity is 100 MVA. The power production of the wind farm is 180 MW, the PCC voltage of both ends is 110 kV and the damping resistor  $R_a = 0.6$  pu. The simulation time span is 20 s. Comparison is made with PI double closed-loop control and passivity control, and the outer-loop PI control parameters of both are identical so as to ensure comparative analysis valid. Fig.5 to Fig.8 shows the steady simulation results.

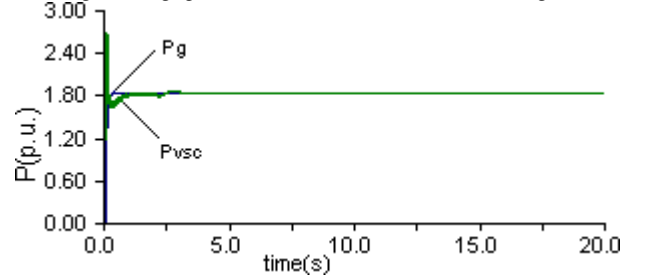


(a) Voltage pu value in PCC under PI double closed-loop control

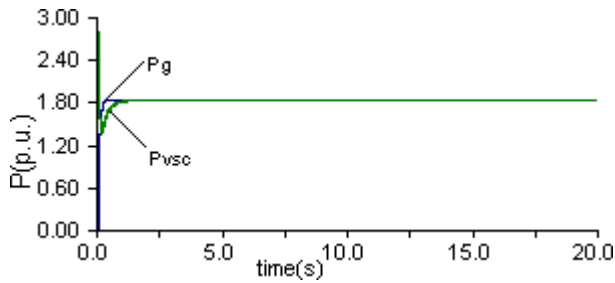


(b) Voltage pu value in PCC under passivity control

Fig.5 Voltage pu value in PCC under two control strategies



(a) Generated power and transmitted power under PI double closed-loop control



(b) Generated power and transmitted power under passivity control

Fig.6 Generated power and transmitted power under two control strategies

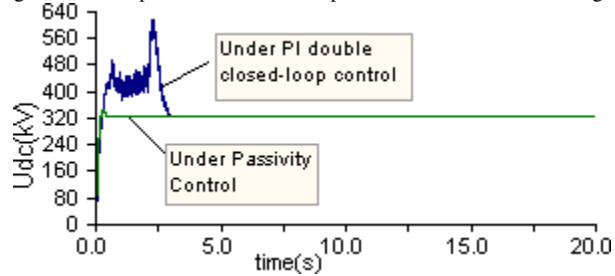
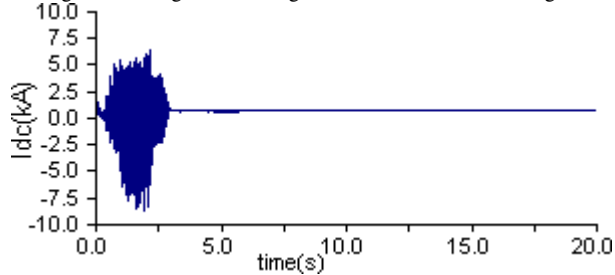
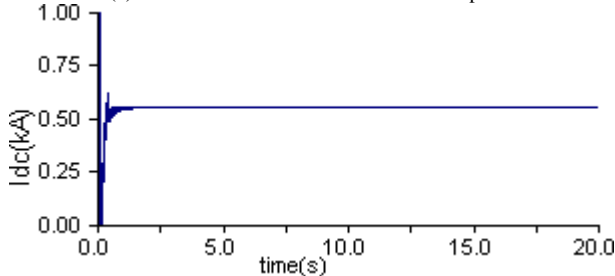


Fig.7 DC voltage of receiving end under two control strategies



(a) DC current under PI double closed-loop control



(b) DC current under passivity control

Fig.8 DC current under two control strategies

Simulation results in Fig.5(b), Fig.6(b), Fig.7 and Fig8(b) show that AC voltage, wind power production, active power transmitted, DC voltage and DC current reach set value quickly and keep stable, no oscillation and very small overshoot under passivity control. Comparison with PI control demonstrate that passivity control make the system have stronger robustness.

In order to compare dynamic response performances, make the wind speed have a step change at 10s and 15s under both control mode, as shown in Fig.9, and Fig.10 to Fig.13 show the simulation results of each variable.

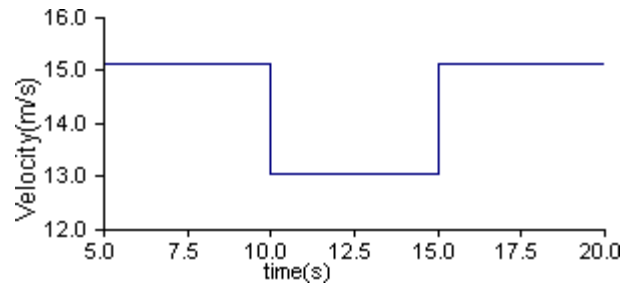
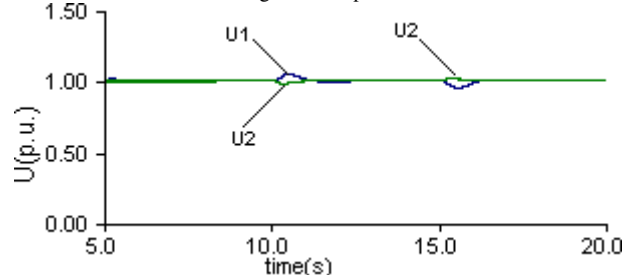
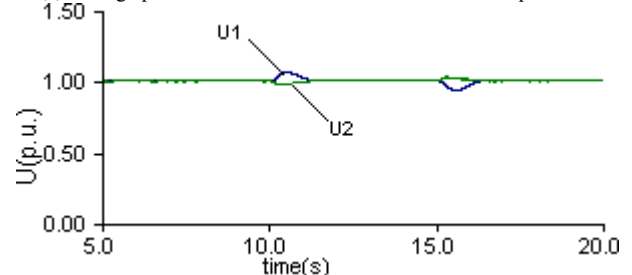


Fig.9 Wind speed

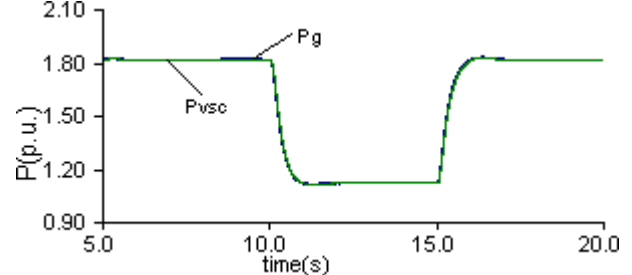


(a) Voltage pu value in PCC under PI double closed-loop control

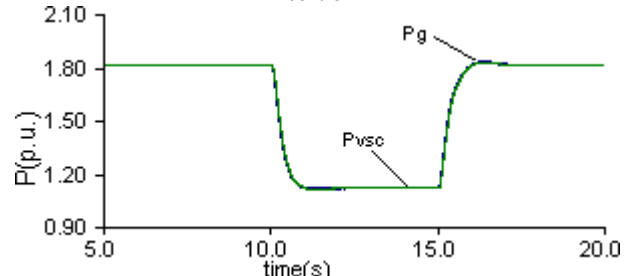


(b) Voltage pu value in PCC under passivity control

Fig.10 Voltage pu value in PCC under step wind disturbance

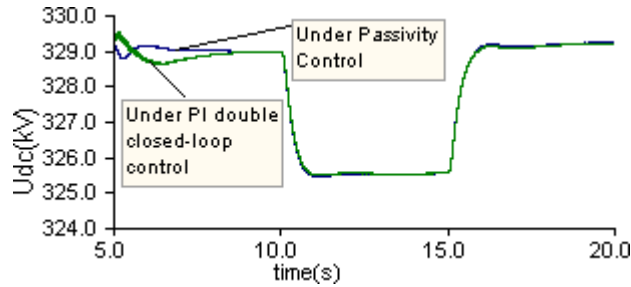


(a) Generated power and transmitted power under PI double closed-loop control

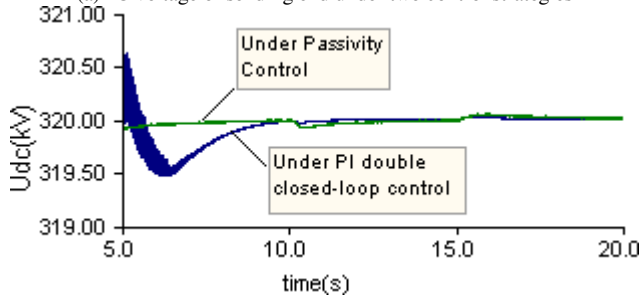


(b) Generated power and transmitted power under passivity control

Fig.11 Generated power and transmitted power under step wind disturbance

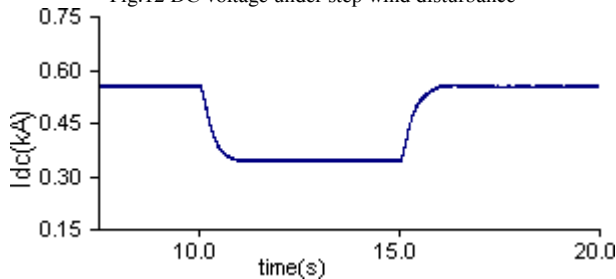


(a) DC voltage of sending end under two control strategies

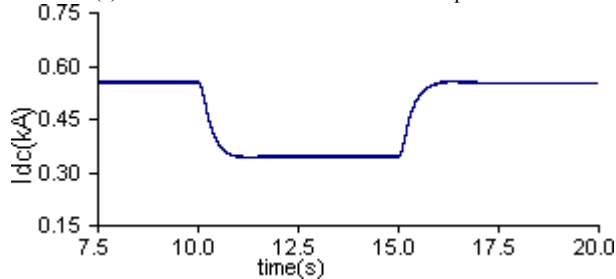


(b) DC voltage of receiving end under two control strategies

Fig.12 DC voltage under step wind disturbance



(a) DC current under PI double closed-loop control



(b) DC current under passivity control

Fig.13 DC current under step wind disturbance

The simulation results show that the AC voltage at both ends PCC have a little fluctuation change and reach stability quickly when wind speed step up or down under both control strategies, as shown in Fig.10. The power transmitted by VSC-HVDC is consistent with the wind power production which changes with wind speed changes, and the transmission link remains stable even if power changes with  $\pm 60$  MW, as shown in Fig.11. Fig.12(a) shows the DC voltage at sending end changes with wind speed changes, but the fluctuation is little and flutter is smaller under passivity control. The receiving end DC voltage is stabilized on set value and error is  $\pm 0.05$  kV under passivity control, but it fluctuates greatly and need much time to reach stability under PI double closed-loop control, as shown in Fig.12(b). In addition, the DC current changes with transmitted power changes, but its ripple is little under passivity control, as shown in Fig.13.

Setting the voltage amplitude step change at the coupling

point of receiving end to simulate voltage disturbance of connected grid, as shown in Fig.14. Fig.15 and Fig.16 shows the results.

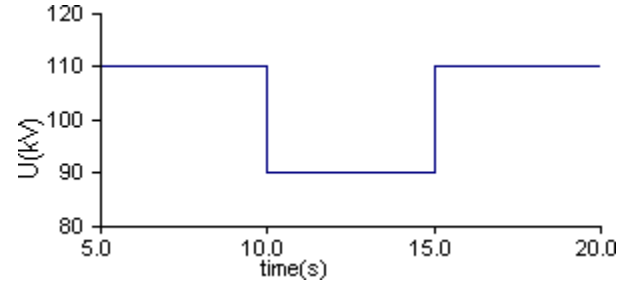
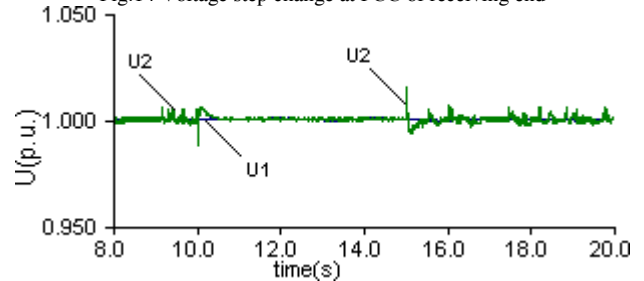
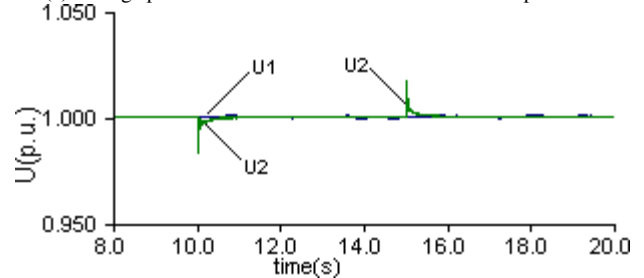


Fig.14 Voltage step change at PCC of receiving end



(a) Voltage pu value in PCC under PI double closed-loop control



(b) Voltage pu value in PCC under passivity control

Fig.15 Voltage pu value in PCC under step voltage disturbance at access point of receiving end

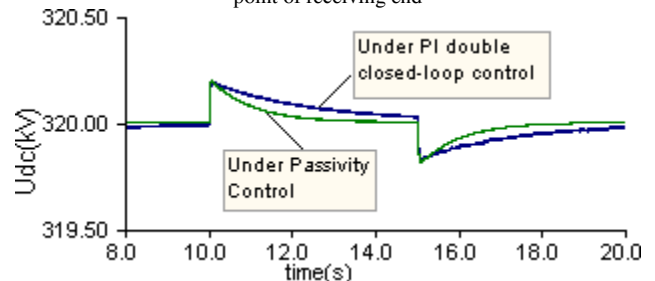


Fig.16 DC voltage of receiving end under step voltage disturbance at access point of receiving end

The AC voltage at both ends is stabilized on expected value and disturbance is admissible when the voltage at access point change, but it has little ripple and better steady performance under passivity control, as shown in Fig.15. As to DC voltage at receiving end, its static error is smaller, recover to set value with quick dynamic response after disturbance under passivity control, as shown in Fig.16.

## VI. CONCLUSION

VSC-HVDC transmission link is a significant scheme to connect large scale wind power. Aiming at the problem of robustness existed in the VSC-HVDC transmission link, a passivity control strategy is proposed for converter in this paper. Error energy storage function is established and used as

Lyapunov function based on the EL mathematical model of converter in d-q rotating coordinates. Based on damping addition, expected equilibrium point, state variable and state error, passivity controller is designed, and decoupled control for every variable is achieved. The proposed model and control strategy are simulated by software PSCAD/EMTDC, and the results shows the control system has good static and dynamic performance and robustness.

#### REFERENCES

- [1] "WWEA. World wind energy report 2010," Shanghai, China, 2011.
- [2] Inigo Martinez de Alegria, Andreu J, José Luis Martín, "Connection requirements for wind farms: A survey on technical requirements and regulation," *Renewable and Sustainable Energy Reviews*, vol. 11, pp. 1858-1872, Oct. 2007.
- [3] Liying Zhang, Tinglu Ye, Yaozhong Xin, et al, "Problems and measures of power grid accommodating large scale wind power," *Proceedings of the CSEE*, vol. 30, pp. 1-9, Sep. 2010.
- [4] Guangfu Tang, Zhiyuan He, Letian Teng, "New progress on HVDC technology based on voltage source converter," *Power System Technology*, vol. 32, pp. 39-42, Nov. 2008.
- [5] Nikolas Flourentzou, Vassilios G. Agelidis, Georgios D. Demetriades, "VSC-based HVDC power transmission systems: an overview," *IEEE Transactions on Power Electronics*, vol. 24, pp. 594-599, Mar. 2009.
- [6] Sheng Jie Shao, Vassilios G. Agelidis, "Review of DC system technologies for large scale integration of wind energy systems with electricity grids," *Energies*, vol. 3, pp. 1303-1319, Jun. 2010.
- [7] S. M. Muyeen, Rion Takahashi, Junji Tamura, "Operation and control of HVDC-connected offshore wind farm," *IEEE Transactions on Sustainable Energy*, vol. 1, pp. 30-37, Apr. 2010.
- [8] ZENG Dan, YAO Jianguo, YANG Shengchun, et al, "Economy comparison of VSC-HVDC with different voltage levels," *Automation of Electric Power Systems*, vol. 35, pp. 98-102, Oct. 2011.
- [9] Bresesti P, Kling W L, Hendriks R L, "HVDC connection of off shore wind farms to the transmission system," *IEEE Transactions on Energy Conversion*, vol. 22, pp. 37-43, Mar. 2007.
- [10] Akshaya Moharana, P.K.Dash, "Input-output linearization and robust sliding-mode controller for the VSC-HVDC transmission link," *IEEE Transactions on Power Delivery*, vol. 25, pp. 1952-1961, Jul. 2010.
- [11] H.F. Latorre, M. Ghandhari, "Improvement of power system stability by using a VSC-HVDC," *Electrical Power and Energy Systems*, vol. 33, pp. 332-333, Feb. 2011.
- [12] Zhang Lidong, Harnefors L, Nee H P, "Interconnection of two very weak AC systems by VSC-HVDC links using power synchronization control," *IEEE Transactions on Power Systems*, vol. 26, pp. 345-347, Feb. 2011.
- [13] Sixiang Yang, Guojie Li, Siye Ruan, "Control strategies for VSC-HVDC applied to DFIG based wind farm," *Automation of Electric Power Systems*, vol. 31, pp. 65-67, Oct. 2007.
- [14] Minyuan Guan, Zheng Xu, "Modeling and control of modular multilevel converter in HVDC transmission," *Automation of Electric Power Systems*, vol. 34, pp. 64-68, Oct. 2010.
- [15] Siye Ruan, Guojie LI, Xiaohong JIAO, et al, "Adaptive control design for VSC-HVDC systems based on backstepping method," *Electric Power Systems Research*, vol. 77, pp. 559-565, Apr. 2007.
- [16] Shuhui Li, Timothy A. Haskew, Ling Xu, "Control of HVDC light system using conventional and direct current vector control approaches," *IEEE Transactions on Power Electronics*, vol. 25, pp. 3106-3118, Dec. 2010.
- [17] LI Shuang, WANG Zhixin, WANG Guoqiang, et al, "PID neural network sliding-mode controller for three-level offshore wind power VSC-HVDC converter," *Proceedings of the CSEE*, vol. 32, pp. 20-28, Feb. 2012.
- [18] Ortega R, Loria A, Nicklasson P J, et al, *Passivity-Based Control of Euler-Lagrange Systems: Mechanical, Electrical and Electromechanical Applications*. London: Springer-verlag London Limited, 1998.
- [19] Lee Tzann Shin, "Lagrangian modeling and passivity based control of three-phase AC/DC voltage-source converters," *IEEE Transaction on Industrial Electronics*, vol. 51, pp. 892-902, Aug. 2004.
- [20] Jiuhe Wang, Lipei Huang, Xiuyuan Yang, "Power control of three-phase boost-type PWM rectifier based on passivity," *Proceedings of the CSEE*, vol. 28, pp. 20-25, Jul. 2008.
- [21] Jinning Yang, Wenming Liu, Shiwei Zhao, et al, "Position control of linear switched reluctance motor using passivity-based control," *Transactions of China Electrotechnical Society*, vol. 25, pp. 56-61, Sep. 2010.
- [22] Yuanzhang Sun, Xiaohong Jiao, Tielon Shen, *Nonlinear Robustness Control of Power System*. BeiJing: Tsinghua University Press, 2007, pp.11-17.



**Xinming Fan** was born in Nankang City in the People's Republic of China, on December 30, 1977. He received the M.S. degree in electrical engineering from South China University of Technology, Guangzhou, China, in 2007. He is currently working toward the Ph.D. degree at South China University of Technology.

His research interest include power system operation analysis and stability control, renewable energy conversion, and VSC-HVDC transmission.

**Lin Guan** was born in 1970 in Xiaogang city, Hubei Province, China. She received the Ph.D degree in electrical engineering from Huazhong University of Science and Technology, Wuhan, China, in 1995. She is currently a Professor and Doctorial Supervisor of Power System and its Automation in the School of Electric Power, South China University of Technology. Her research interests include power system operation, power system stability and control, planning and reliability, artificial intelligence and its application in power system.

Prof. Guan presided national natural science fund projects, Guangdong province natural science fund projects and electric power enterprise research projects and sums over 20. She was awarded many provincial prizes such as the First Prize of Hubei Province Natural Science, the Second Prize of China University Science and Technology of Ministry of Education, et al. She published 50 papers in IEEE Transactions, IEE Proceeding G.T.D and domestic important journals, among them 30 papers were indexed by SCI and EI.

**Chengjun Xia** was born in 1974 in Huanggang city, Hubei Province, China. He received the Ph.D degree in electrical engineering from Huazhong University of Science and Technology, Wuhan, China, in 2003. He is currently a Associate Professor and Master Tutor of Power System and its Automation in the School of Electric Power, South China University of Technology. His research interests include power system operation, power system stability and control, planning and reliability.

**Jianming He** was born in 1988. He received his bachelor degree in electrical engineering from Huazhong University of Science and Technology, Wuhan, China, in 2010. He is currently master candidate at South China University of Technology. His research interest include power system operation analysis and stability control, renewable energy conversion.